Fullerene Radicals

International Edition: DOI: 10.1002/anie.201511930
German Edition: DOI: 10.1002/ange.201511930

Crystallographic Evidence for Direct Metal–Metal Bonding in a Stable Open-Shell $La_2@I_h$-C_{80} Derivative

*Lipiao Bao, Muqing Chen, Changwang Pan, Takahisa Yamaguchi, Tatsuhisa Kato, Marilyn M. Olmstead, Alan L. Balch, Takeshi Akasaka, and Xing Lu**

Dedicated to Professor Zhennan Gu on the occasion of his 80th birthday

Abstract: *Endohedral metallofullerenes (EMFs) have novel structures and properties that are closely associated with the internal metallic species. Benzyl radical additions have been previously shown to form closed-shell adducts by attaching an odd number of addends to open-shell EMFs (such as $Sc_3C_2@I_h$-C_{80}) whereas an even number of groups are added to closed-shell EMFs (for example $Sc_3N@I_h$-C_{80}). Herein we report that benzyl radical addition to the closed-shell $La_2@I_h$-C_{80} forms a stable, open-shell monoadduct instead of the anticipated closed-shell bisadduct. Single-crystal X-ray diffraction results show the formation of a stable radical species. In this species, the La–La distance is comparable to the theoretical value of a La–La covalent bond and is shorter than reported values for other $La_2@I_h$-C_{80} derivatives, providing unambiguous evidence for the formation of direct La–La bond.*

Encapsulation of metal atoms or metal clusters inside fullerene cages affords a collection of novel molecules, which are called endohedral metallofullerenes (EMFs).[1–4] The charge transfer from the internal unit to the fullerene cage gives rise to the important properties of EMFs. Based on the charge localized on the fullerene cage, two types of EMFs could be identified: open-shell EMFs with an unpaired electron residing on the cage or closed-shell EMFs containing only paired electrons. Significantly, open-shell EMFs have a high reactivity toward radical reactions because of their own radical character. For instance, several insoluble mono-EMFs such as $La@C_{2n}$ ($2n = 72$, 74, 80, 82)[5–9] were solubilized during a 1,2,4-trichlorobenzene extraction process. The discovery of these insoluble EMFs was achieved because these highly reactive, open-shell EMFs can be transformed into stable, closed-shell derivatives through radical coupling reactions with dichlorophenyl radicals. Additionally, the reaction between $La@C_{82}$ and toluene[10] also revealed that the open-shell $La@C_{82}$ is able to convert into a closed-shell derivative. Similarly, an unexpected NO_2 radical addition occurred when anthranilic acid and isoamyl nitrite reacted with $La@C_{82}$.[11] The CF_3 radical generated by thermolysis of CF_3I or $Ag(CF_3CO_2)$ can be readily attached to EMFs. Trifluoromethylation of EMFs was firstly carried out on the open-shell $Y@C_{82}$ to afford a series of closed-shell adducts $Y@C_{82}(CF_3)_n$ ($n = 1$, 3, 5)[12] with an odd number of addends. Further examples include a collection of $Sc_3N@C_{80}(CF_3)_{2n}$ molecules[13–16] and trifluoromethylated derivatives of empty fullerenes such as C_{60}, C_{70}, and C_{84}.[12,17–26] In these adducts an even number of CF_3 radicals was always attached to these fullerenes to maintain their closed-shell configurations. However, CF_3 addition normally provides mixtures with multiple CF_3 groups added to the carbon cage. Thus, polyaddition limits the applications of this reaction and new radical reactions with high selectivity are desirable.

Recently, the benzyl radical, generated from benzyl bromide (**1**) under photoirradiation, has attracted increasing attention owing to its high regioselectivity when reacting with fullerenes. For instance, only one monoadduct is formed upon reacting the benzyl radical with the open-shell $Sc_3C_2@I_h$-C_{80}.[27] Benzylation of closed-shell C_{60} formed either a bisadduct[28] or monoadduct that underwent a dimerization to stabilize the unpaired electron through C–C bond formation.[29] Likewise, attachment of benzyl radicals to the closed-shell $Sc_3N@I_h$-C_{80} yielded exclusively a bisadduct.[30] With this information in hand, it can be concluded that an odd number of benzyl radicals will be added to open-shell EMFs whereas an even number of radicals will be added to closed-shell EMFs to obtain adducts with closed-shell configurations. However, this dogma is broken here in the reaction of the benzyl radical with the closed-shell $La_2@I_h$-C_{80}, which affords an open-shell, monoadduct $La_2@I_h$-$C_{80}(C_7H_7)$ (**2**) regioselectively. Crystallographic, EPR spectroscopic, and theoretical results reveal that the La_2 cluster inside the cage accepts an

[*] L. Bao, Dr. M. Chen, C. Pan, Prof. T. Akasaka, Prof. X. Lu
State Key Laboratory of Materials Processing and Die and Mold Technology, School of Materials Science and Engineering
Huazhong University of Science and Technology
1037, Luoyu Road, Wuhan 430074 (P.R. China)
E-mail: lux@hust.edu.cn
T. Yamaguchi, Prof. T. Kato
Graduate School of Human and Environmental Sciences
Kyoto University, Kyoto, 606-8501 (Japan)
Prof. T. Kato
Institute for Liberal Arts and Sciences, Kyoto University
Kyoto, 606-8501 (Japan)
Prof. M. M. Olmstead, Prof. A. L. Balch
Department of Chemistry, University of California, Davis
Davis, CA 95616 (USA)
Prof. T. Akasaka
Foundation for Advancement of International Science
Tsukuba, 30–0821 (Japan)

Supporting information for this article can be found under http://dx.doi.org/10.1002/anie.201511930.

unpaired electron by forming a metal–metal bond and stabilizing the fullerene radical species.

Typically, a toluene solution of $La_2@I_h$-C_{80} and benzyl bromide (**1**) was irradiated with light of wavelength $\lambda >$ 350 nm under argon. The reaction process was monitored by HPLC (Figure 1). Before irradiation, peaks for **1** and $La_2@I_h$-C_{80} were detected at 3.4 min and 25.0 min, respectively. After irradiation for 1 h, a new peak appeared at 11.9 min, which was assigned as the monoadduct **2** (see below). HPLC separation gave pure product **2** in a high yield (circa 90%) based on consumed $La_2@I_h$-C_{80}.

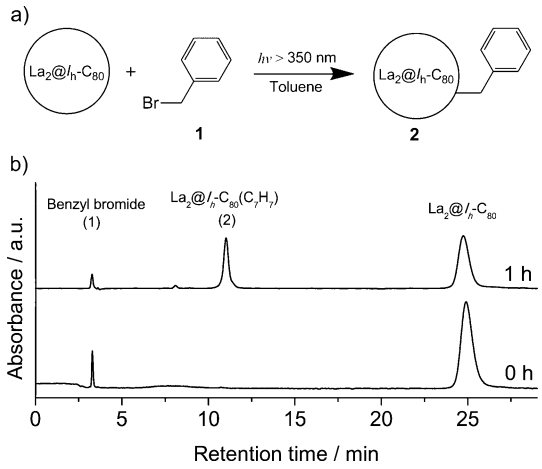

Figure 1. a) The reaction between $La_2@I_h$-C_{80} and benzyl bromide (**1**). b) HPLC profiles of the reaction mixture probed at different times. HPLC conditions: 5PYE column (4.6 mm × 250 mm), 20 μL injection volume, 1.0 mL min^{-1} toluene flow, RT, $\lambda = 330$ nm UV detector.

The matrix-assisted laser desorption/ionization time-of-flight mass spectrum (MALDI-TOF MS) of **2** shows a strong signal at m/z 1329 (Figure 2), which corresponds to a 1:1 adduct. The observed isotopic distribution of **2** agrees well with the calculated result. The peak at m/z 1238, ascribed to $La_2@I_h$-C_{80}, was generated by detachment of the benzyl moiety from **2** under laser irradiation.

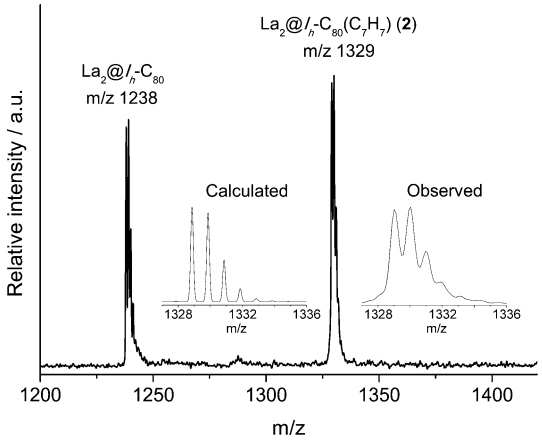

Figure 2. MALDI-TOF mass spectrum of **2** recorded under a negative linear mode.

The electronic configuration of **2** was investigated by visible/NIR absorption spectroscopy. The relatively featureless spectrum of pristine $La_2@I_h$-C_{80}, shown in Figure 3, changes considerably upon attachment of the benzyl moiety, with the spectrum of compound **2** having new absorption bands at $\lambda = 677$ nm and 850 nm. This change in the absorption spectra can probably be attributed to the effect of the unpaired electron in this fullerene radical. Undoubtedly, the electronic structure of $La_2@I_h$-C_{80} has been altered markedly by the benzylation reaction.

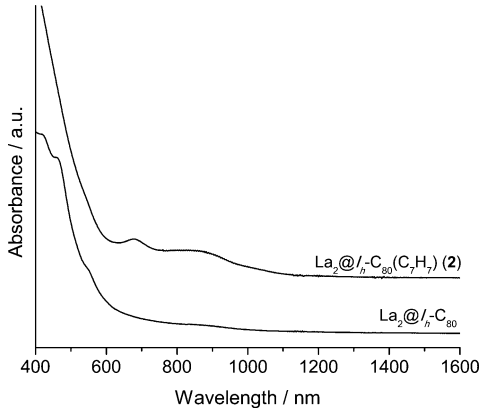

Figure 3. Vis/NIR absorption spectra of $La_2@I_h$-C_{80} and $La_2@I_h$-C_{80}-(C_7H_7) (**2**) in toluene. The two curves are vertically shifted for ease of comparison.

The electrochemical properties of **2** were investigated by cyclic voltammetry (CV) and differential pulse voltammetry (DPV) measurements. Compound **2** exhibits one oxidation process and five reduction steps (see Figure S1 in the Supporting Information). Table 1 lists the electrochemical potentials of **2** and $La_2@I_h$-C_{80}.[31] Compared with the corresponding values of pristine $La_2@I_h$-C_{80}, the first oxidation potential of **2** is negatively shifted by 410 mV, but the first reduction potential is negatively shifted by 510 mV. Accordingly, the electrochemical gap of **2** (0.97 V) is slightly larger than that of pristine $La_2@I_h$-C_{80} (0.87 V).

Table 1: Redox potentials (V versus Fc/Fc^+) of **2** and $La_2@I_h$-C_{80}.[a]

Compound	$^{ox}E_1$	$^{red}E_1$	$^{red}E_2$	$^{red}E_3$	$^{red}E_4$	$^{red}E_5$
2	0.15	−0.82	−1.34	−1.64	−1.90	−2.28
$La_2@I_h$-C_{82}[b]	0.56	−0.31	−1.71	−2.13	–	–

[a] Determined by differential pulse voltammetry in 1,2-dichlorobenzene with 0.1 M $(n\text{-Bu})_4NPF_6$ at a Pt working electrode. [b] Data from Ref. [31].

The molecular structure of **2** was determined by single-crystal X-ray diffraction.[46] The asymmetric unit contains an entire molecule of **2** and two disordered CS_2 molecules. Both the fullerene cage and the benzyl unit show three orientations with respective occupancy values of 0.41, 0.36, and 0.23. Figure 4 shows the major components of **2**. The benzyl addition occurs at one of the [5,6,6]-junction carbon atoms of I_h-C_{80}, which are more pyramidalized than the [6,6,6]-junction

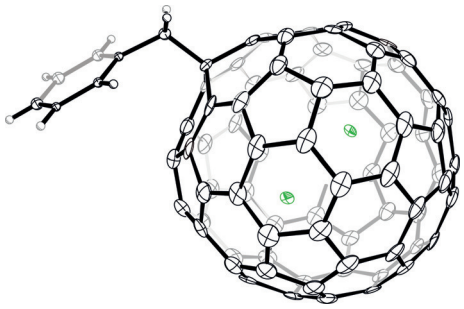

Figure 4. ORTEP drawing of $La_2@I_h$-$C_{80}(C_7H_7)$ (**2**) with thermal ellipsoids set at 30% probability. Only the major cage orientation (0.41 occupancy) and the metal sites, La1 and La2 (shown in green), are shown. Solvent molecules were omitted for clarity.

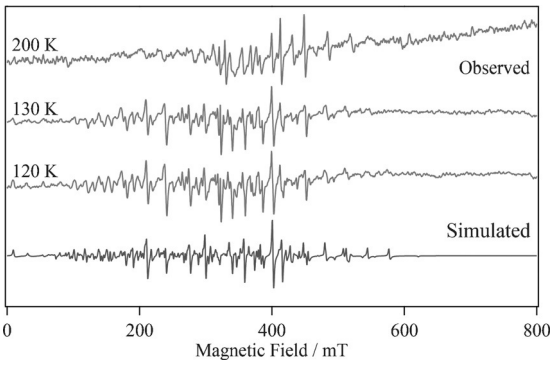

Figure 5. Simulated and observed EPR spectra of $La_2@I_h$-$C_{80}(C_7H_7)$ (**2**). The observed spectra (upper three) were recorded at 120 K, 130 K, and 200 K, respectively. The simulated spectrum (bottom) was recorded using the parameters: g tensor (1.840, 1.840, 1.980), ^{139}La HFI tensor (31.7, 31.7, 43.1) mT, and linewidth $\Delta H_{pp} = 2.5$ mT.

carbon atoms.[2] Surprisingly, only one benzyl moiety is attached to the cage, in sharp contrast to the addition of two benzyl radicals to $Sc_3N@I_h$-C_{80}.[30] Moreover, no dimerization occurs in the crystalline state. In contrast, the monoadduct formed by benzylation of C_{60} is a dimer in its crystal form.[29]

Inside the cage, the two La atoms can move freely, resulting in up to 17 disordered sites with occupancies varying from 0.02 to 0.22, whereas the distances between the two La atoms range from 3.779 Å to 3.676 Å. Notably, the mean La–La distance (3.71 Å; with an average deviation from the mean of 0.04 Å) is comparable to the calculated La–La covalent bond length (3.723 Å) in the $La_2@I_h$-C_{80}^- anion,[32] thus presenting clear experimental evidence of direct metal–metal bonding inside **2**. In addition, this La–La distance is much shorter (by 0.04–0.449 Å) than the values in pristine $La_2@I_h$-C_{80} and any other $La_2@I_h$-C_{80} derivatives[33–41] (Table 2), which further confirms the formation of the metal–metal bond.

The paramagnetic nature and the occurrence of metal–metal bonding in **2** were further verified by EPR spectroscopy. The X-band EPR signal of **2** (Figure 5) resembles that of the $La_2@I_h$-C_{80} anion radical.[41] In this context, the unpaired electron is not distributed on the carbon cage but is mainly confined to the internal La–La σ-bonding orbital. A similar situation occurs in the case of the $Sc_3N@C_{80}$ radical anion in which the spin is also transferred from the cage to the internal cluster.[42] The simulation by the large ^{139}La hyperfine interaction (HFI) with the doublet electron spin ($S = 1/2$) reproduces well the spectra recorded at 120 K, 130 K, and 200 K. The spectra were reproduced by using the tetragonal (axially symmetric) g tensor (($g_x = g_y$, g_z) = (1.840, 1.980)) and ^{139}La HFI tensor (($A_x = A_y$, A_z) = (31.7, 43.1) mT) parameters. After the frozen solution was melted at 200 K, the magnetic-field-dependent linewidth of the spectrum broadened the lines of some transitions beyond detectability. The simulation parameters reveal two important pieces of information: first, the two La ions are identical in terms of ESR parameters; and second, the tensors are tetragonal (axially symmetric). The latter observation is confirmed by the result that no split x and y anisotropic component is seen in the magnetic field from 200 to 400 mT. Estimating from the linewidth, the anisotropic x and y components would be averaged by the rotation with the correlation time of circa 0.01 μs. The fact that the La ions are identical in terms of ESR parameters was reflected by the alternation of two La ions within the cage, which readily makes the spin density on two La ions equal.

Theoretical studies of the spin-density distribution of **2** were conducted to explain the spin states of **2**. Previous results have revealed that the lowest unoccupied molecular orbital (LUMO) of $La_2@I_h$-C_{80} is localized on the La–La σ-bonding orbital and as a consequence, an unpaired electron could be confined to the La_2 cluster rather than on the fullerene cage.[31,41,43–45] As depicted in Figure 6, density functional theory (DFT) calculations reveal that the singly occupied molecule orbital (SOMO) of **2** is predominately localized on the La_2 pair, a situation that is consistent with a previous report about the $La_2@I_h$-C_{80} anion,[32] and confirms the metal–metal bonding between the two La ions. In agreement with the EPR data, the spin densities of the two La ions were calculated to be 0.460 and 0.467, suggesting that the unpaired electron was localized on the La_2 cluster rather than on the fullerene cage, a factor that is responsible for the high stability of the fullerene radical **2**. These results have not only clarified the chemical stability of **2** but have also explained the formation of only the monoadduct in the reaction between

Table 2: Average La–La distances [Å] of $La_2@I_h$-C_{80} and its derivatives from X-ray crystallographic data.[a]

Compound	La–La distance [Å]	Reference
2	3.71	This work
$La_2@I_h$-$C_{80}(C_3N_3Ph_2)$	3.750	[41]
$La_2@I_h$-$C_{80}(Dep_2Si)_2CH_2$	3.793	[36]
$La_2@I_h$-$C_{80}[SiDep_2(CH_2)CHtBp]$	3.808	[38]
$La_2@I_h$-C_{80}(TCNEO)	3.814	[40]
$La_2@I_h$-$C_{80}(CH_2)$NTrt	3.823	[34, 35]
$La_2@I_h$-C_{80}	3.840	[33]
$La_2@I_h$-C_{80}(CPhCl)	4.013	[39]
$La_2@I_h$-C_{80}(Ad)	4.031	[37]
$La_2@I_h$-C_{80}(CPhCl)(Ad)	4.159	[39]

[a] Dep = 2,6-diethylphenyl; tBp = 4-*tert*-butylphenyl; TCNEO = tetracyanoethylene oxide; Trt = triphenylmethyl; Ad = adamantylidene.

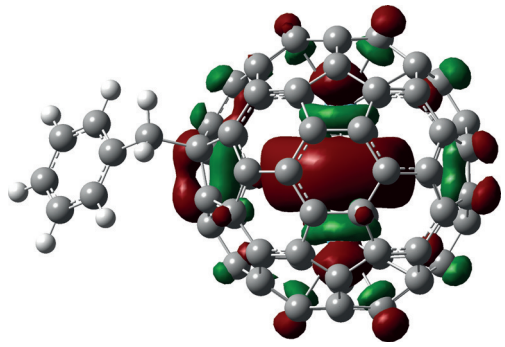

Figure 6. SOMO isoelectronic plot of **2** calculated at the B3LYP/6-31G(d) ≈ sdd level.

benzyl radical and $La_2@I_h$-C_{80}. Additionally, the energy diagram of **2** (Figure S2) demonstrates that the SOMO of **2** (−4.83 eV) lies in between the highest occupied molecular orbital (HOMO; −5.70 eV) and the LUMO (−4.55 eV) of pristine $La_2@I_h$-C_{80},[43] suggesting its high stability.

In summary, a stable fullerene radical $La_2@I_h$-$C_{80}(C_7H_7)$ (**2**) was synthesized by the regioselective reaction of benzyl bromide (**1**) with $La_2@I_h$-C_{80} and was fully characterized by a collection of experimental and theoretical methods. Although the same I_h-C_{80} cage is present in $Sc_3N@I_h$-C_{80}, $Sc_3C_2@I_h$-C_{80}, and $La_2@I_h$-C_{80}, closed-shell benzylation derivatives were obtained for $Sc_3N@I_h$-C_{80} and $Sc_3C_2@I_h$-C_{80} whereas an open-shell monoadduct was formed for $La_2@I_h$-C_{80}. EPR studies and DFT calculations reveal that the La_2 cluster can accept the unpaired electron into their σ-bonding orbital to stabilize the open-shell fullerene radical **2**. The short La–La distance, which is comparable to the theoretical value for a La–La single bond, is indicative of metal–metal bonding. Furthermore, electrochemical measurements demonstrate a larger electrochemical gap for **2** than pristine $La_2@I_h$-C_{80}. Our results reveal that the unpaired electron from the exohedral unit can be transferred to the internal metallic cluster through the strong metal–cage interactions, a feature that may provide valuable clues to the design and creation of single-molecule magnets.

Acknowledgements

Financial support from The National Thousand Talents Program of China, NSFC (Nos. 21171061 and 51472095), the Program for Changjiang Scholars and Innovative Research Team in University (IRT1014), Key Laboratory of Functional Inorganic Material Chemistry (Heilongjiang University), and the US National Science Foundation, (Grant CHE-1305125 to A.L.B. and M.M.O.) is gratefully acknowledged. We thank the Advanced Light Source, supported by the Director, Office of Science, Office of Basic Energy Sciences, of the U.S. Department of Energy under Contract No. DE-AC02-05CH11231, for beam time, and the Analytical and Testing Center in Huazhong University of Science and Technology for all related measurements.

Keywords: density functional calculations · endohedral fullerenes · metal–metal bonding · radical reactions · structure elucidation

How to cite: *Angew. Chem. Int. Ed.* **2016**, *55*, 4242–4246
Angew. Chem. **2016**, *128*, 4314–4318

[1] X. Lu, L. Feng, T. Akasaka, S. Nagase, *Chem. Soc. Rev.* **2012**, *41*, 7723–7760.
[2] X. Lu, L. Bao, T. Akasaka, S. Nagase, *Chem. Commun.* **2014**, *50*, 14701–14715.
[3] A. Popov, S. Yang, L. Dunsch, *Chem. Rev.* **2013**, *113*, 5989–6113.
[4] X. Lu, L. Echegoyen, A. L. Balch, S. Nagase, T. Akasaka, *Endohedral Metallofullerenes: Basics and Applications*, CRC Press, **2014**.
[5] T. Wakahara, H. Nikawa, T. Kikuchi, T. Nakahodo, G. M. A. Rahman, T. Tsuchiya, Y. Maeda, T. Akasaka, K. Yoza, E. Horn et al., *J. Am. Chem. Soc.* **2006**, *128*, 14228–14229.
[6] H. Nikawa, T. Kikuchi, T. Wakahara, T. Nakahodo, T. Tsuchiya, G. M. A. Rahman, T. Akasaka, Y. Maeda, K. Yoza, E. Horn et al., *J. Am. Chem. Soc.* **2005**, *127*, 9684–9685.
[7] X. Lu, H. Nikawa, K. Kikuchi, N. Mizorogi, Z. Slanina, T. Tsuchiya, T. Akasaka, S. Nagase, *Angew. Chem. Int. Ed.* **2011**, *50*, 6356–6359; *Angew. Chem.* **2011**, *123*, 6480–6483.
[8] H. Nikawa, T. Yamada, B. P. Cao, N. Mizorogi, Z. Slanina, T. Tsuchiya, T. Akasaka, K. Yoza, S. Nagase, *J. Am. Chem. Soc.* **2009**, *131*, 10950–10954.
[9] T. Akasaka, X. Lu, H. Kuga, H. Nikawa, N. Mizorogi, Z. Slanina, T. Tsuchiya, K. Yoza, S. Nagase, *Angew. Chem. Int. Ed.* **2010**, *49*, 9715–9719; *Angew. Chem.* **2010**, *122*, 9909–9913.
[10] Y. Takano, A. Yomogida, H. Nikawa, M. Yamada, T. Wakahara, T. Tsuchiya, M. O. Ishitsuka, Y. Maeda, T. Akasaka, T. Kato et al., *J. Am. Chem. Soc.* **2008**, *130*, 16224–16230.
[11] X. Lu, H. Nikawa, T. Tsuchiya, T. Akasaka, M. Toki, H. Sawa, N. Mizorogi, S. Nagase, *Angew. Chem. Int. Ed.* **2010**, *49*, 594–597; *Angew. Chem.* **2010**, *122*, 604–607.
[12] I. E. Kareev, I. V. Kuvychko, S. F. Lebedkin, S. M. Miller, O. P. Anderson, K. Seppelt, S. H. Strauss, O. V. Boltalina, *J. Am. Chem. Soc.* **2005**, *127*, 8362–8375.
[13] N. B. Shustova, Y. S. Chen, M. A. Mackey, C. E. Coumbe, J. P. Phillips, S. Stevenson, A. A. Popov, O. V. Boltalina, S. H. Strauss, *J. Am. Chem. Soc.* **2009**, *131*, 17630–17637.
[14] N. B. Shustova, D. V. Peryshkov, I. V. Kuvychko, Y. S. Chen, M. A. Mackey, C. E. Coumbe, D. T. Heaps, B. S. Confait, T. Heine, J. P. Phillips et al., *J. Am. Chem. Soc.* **2011**, *133*, 2672–2690.
[15] N. B. Shustova, A. A. Popov, M. A. Mackey, C. E. Coumbe, J. P. Phillips, S. Stevenson, S. H. Strauss, O. V. Boltalina, *J. Am. Chem. Soc.* **2007**, *129*, 11676–11677.
[16] A. A. Popov, N. B. Shustova, A. L. Svitova, M. A. Mackey, C. E. Coumbe, J. P. Phillips, S. Stevenson, S. H. Strauss, O. V. Boltalina, L. Dunsch, *Chem. Eur. J.* **2010**, *16*, 4721–4724.
[17] A. A. Popov, I. E. Kareev, N. B. Shustova, E. B. Stukalin, S. F. Lebedkin, K. Seppelt, S. H. Strauss, O. V. Boltalina, L. Dunsch, *J. Am. Chem. Soc.* **2007**, *129*, 11551–11568.
[18] S. I. Troyanov, A. A. Goryunkov, N. B. Tamm, V. Y. Markov, I. N. Ioffe, L. N. Sidorov, *Dalton Trans.* **2008**, 2627–2632.
[19] I. E. Kareev, G. S. Quinones, I. V. Kuvychko, P. A. Khavrel, I. N. Ioffe, I. V. Goldt, S. F. Lebedkin, K. Seppelt, S. H. Strauss, O. V. Boltalina, *J. Am. Chem. Soc.* **2005**, *127*, 11497–11504.
[20] I. E. Kareev, N. B. Shustova, D. V. Peryshkov, S. F. Lebedkin, S. M. Miller, O. P. Anderson, A. A. Popov, O. V. Boltalina, S. H. Strauss, *Chem. Commun.* **2007**, 1650–1652.
[21] A. A. Popov, N. B. Shustova, O. V. Boltalina, S. H. Strauss, L. Dunsch, *ChemPhysChem* **2008**, *9*, 431–438.
[22] I. E. Kareev, I. V. Kuvychko, A. A. Popov, S. F. Lebedkin, S. M. Miller, O. P. Anderson, S. H. Strauss, O. V. Boltalina, *Angew.*

Chem. Int. Ed. **2005**, *44*, 7984 – 7987; *Angew. Chem.* **2005**, *117*, 8198 – 8201.
[23] A. A. Popov, I. E. Kareev, N. B. Shustova, S. E. Lebedkin, S. H. Strauss, O. V. Boltalina, L. Dunsch, *Chem. Eur. J.* **2008**, *14*, 107 – 121.
[24] I. E. Kareev, I. V. Kuvychko, N. B. Shustova, S. F. Lebedkin, V. P. Bubnov, O. P. Anderson, A. A. Popov, O. V. Boltalina, S. H. Strauss, *Angew. Chem. Int. Ed.* **2008**, *47*, 6204 – 6207; *Angew. Chem.* **2008**, *120*, 6300 – 6303.
[25] I. E. Kareev, A. A. Popov, I. V. Kuvychko, N. B. Shustova, S. F. Lebedkin, V. P. Bubnov, O. P. Anderson, K. Seppelt, S. H. Strauss, O. V. Boltalina, *J. Am. Chem. Soc.* **2008**, *130*, 13471 – 13489.
[26] S. F. Yang, C. B. Chen, T. Wei, N. B. Tamm, E. Kemnitz, S. I. Troyanov, *Chem. Eur. J.* **2012**, *18*, 2217 – 2220.
[27] H. Fang, H. Cong, M. Suzuki, L. Bao, B. Yu, Y. Xie, N. Mizorogi, M. M. Olmstead, A. L. Balch, S. Nagase et al., *J. Am. Chem. Soc.* **2014**, *136*, 10534 – 10540.
[28] W. Si, X. Zhang, N. Asao, Y. Yamamoto, T. Jin, *Chem. Commun.* **2015**, *51*, 6392 – 6394.
[29] W.-W. Yang, Z.-J. Li, X. Gao, *J. Org. Chem.* **2011**, *76*, 6067 – 6074.
[30] C. Shu, C. Slebodnick, L. Xu, H. Champion, T. Fuhrer, T. Cai, J. E. Reid, W. Fu, K. Harich, H. C. Dorn et al., *J. Am. Chem. Soc.* **2008**, *130*, 17755 – 17760.
[31] T. Suzuki, Y. Maruyama, T. Kato, K. Kikuchi, Y. Nakao, Y. Achiba, K. Kobayashi, S. Nagase, *Angew. Chem. Int. Ed. Engl.* **1995**, *34*, 1094 – 1096; *Angew. Chem.* **1995**, *107*, 1228 – 1230.
[32] A. A. Popov, L. Dunsch, *Chem. Eur. J.* **2009**, *15*, 9707 – 9729.
[33] E. Nishibori, M. Takata, M. Sakata, A. Taninaka, H. Shinohara, *Angew. Chem. Int. Ed.* **2001**, *40*, 2998 – 2999; *Angew. Chem.* **2001**, *113*, 3086 – 3087.
[34] M. Yamada, T. Wakahara, T. Nakahodo, T. Tsuchiya, Y. Maeda, T. Akasaka, K. Yoza, E. Horn, N. Mizorogi, S. Nagase, *J. Am. Chem. Soc.* **2006**, *128*, 1402 – 1403.
[35] M. Yamada, M. Okamura, S. Sato, C. I. Someya, N. Mizorogi, T. Tsuchiya, T. Akasaka, T. Kato, S. Nagase, *Chem. Eur. J.* **2009**, *15*, 10533 – 10542.
[36] T. Wakahara, M. Yamada, S. Takahashi, T. Nakahodo, T. Tsuchiya, Y. Maeda, T. Akasaka, M. Kako, K. Yoza, E. Horn et al., *Chem. Commun.* **2007**, 2680 – 2682.
[37] M. Yamada, C. Someya, T. Wakahara, T. Tsuchiya, Y. Maeda, T. Akasaka, K. Yoza, E. Horn, M. T. H. Liu, N. Mizorogi et al., *J. Am. Chem. Soc.* **2008**, *130*, 1171 – 1176.
[38] M. Yamada, M. Minowa, S. Sato, M. Kako, Z. Slanina, N. Mizorogi, T. Tsuchiya, Y. Maeda, S. Nagase, T. Akasaka, *J. Am. Chem. Soc.* **2010**, *132*, 17953 – 17960.
[39] M. O. Ishitsuka, S. Sano, H. Enoki, S. Sato, H. Nikawa, T. Tsuchiya, Z. Slanina, N. Mizorogi, M. T. H. Liu, T. Akasaka et al., *J. Am. Chem. Soc.* **2011**, *133*, 7128 – 7134.
[40] M. Yamada, M. Minowa, S. Sato, Z. Slanina, T. Tsuchiya, Y. Maeda, S. Nagase, T. Akasaka, *J. Am. Chem. Soc.* **2011**, *133*, 3796 – 3799.
[41] M. Yamada, H. Kurihara, M. Suzuki, M. Saito, Z. Slanina, F. Uhlik, T. Aizawa, T. Kato, M. M. Olmstead, A. L. Balch et al., *J. Am. Chem. Soc.* **2015**, *137*, 232 – 238.
[42] P. Jakes, K.-P. Dinse, *J. Am. Chem. Soc.* **2001**, *123*, 8854 – 8855.
[43] M. Yamada, Z. Slanina, N. Mizorogi, A. Muranaka, Y. Maeda, S. Nagase, T. Akasaka, N. Kobayashi, *Phys. Chem. Chem. Phys.* **2013**, *15*, 3593 – 3601.
[44] T. Tsuchiya, M. Wielopolski, N. Sakuma, N. Mizorogi, T. Akasaka, T. Kato, D. M. Guldi, S. Nagase, *J. Am. Chem. Soc.* **2011**, *133*, 13280 – 13283.
[45] T. Kato, *J. Mol. Struct.* **2007**, *838*, 84 – 88.
[46] CCDC 1404316 contains the supplementary crystallographic data for this paper. These data can be obtained free of charge from The Cambridge Crystallographic Data Centre.

Received: December 24, 2015
Published online: February 25, 2016

